Optimization and Control Methods for Ultrasound Surgery

Matti Malinen
Department of Applied Physics, University of Kuopio, P.O. Box 1627, FI-70211 Kuopio, Finland
Matti.Malinen@uku.fi

Tomi Huttunen
Department of Applied Physics, University of Kuopio, P.O. Box 1627, FI-70211 Kuopio, Finland
Tomi.Huttunen@uku.fi

Jari P. Kaipio
Department of Applied Physics, University of Kuopio, P.O.Box 1627, FI-70211 Kuopio, Finland
Jari.Kaipio@uku.fi

Abstract. *When ultrasound propagates in tissue, the wave energy is partially absorbed and turned into heat. In ultrasound surgery the aim is to destroy tumors by heating them with high intensity focused ultrasound. The main advantages of ultrasound surgery are that it is noninvasive and the spatial accuracy is good. The main disadvantage is that the treatment of large tumor volumes is slow with current ultrasound surgery techniques, since healthy tissue between tumor and transducer must be allowed to cool to avoid undesired thermal damage. Therefore, new optimization and control methods are needed to decrease the treatment time by controlling temperature in the cancerous tissue as well as in healthy tissue. In this paper, model based optimization scheme is presented to optimize thermal dose in ultrasound surgery. The method is extended with feedback controller with can be applied during the actual sonication to decrease the effect of the modeling errors.*

Keywords: *Ultrasound, control, optimization, simulation*

1. Introduction

In ultrasound surgery, absorbed energy of the ultrasound wave is used to destroy the cancerous tissue. The temperature in cancerous tissue during such a treatment is raised up to 50-90°C for several seconds (ter Haar, 1995) and (ter Haar 2001). This high temperature results in rapid increase in thermal dose in the focal region. In addition, by using a high temperature the treatment time of small cancer volumes can be decreased and the effect of the diffusion and perfusion can be minimized (Hynynen, 1996). The ultrasound surgery is usually accomplished so that the tumor volume is scanned point by point with individual foci. The scanning is accomplished by changing the position of the transducer or by changing the phase and amplitude of the ultrasound waves which are emitted from several transducer elements. During the treatment, temperature is measured using magnetic resonance imaging (MRI) to get temperature feedback Cline et al. (1993). The scanning method is suitable for treating the small tumor volumes, but in the case of larger volumes the healthy tissue must be allowed to cool to prevent undesired damage of the healthy tissue (ter Haar, 2001). Due to this limitation, the interest for using the more sophisticated optimization and control methods to optimize ultrasound surgery has been increased (Fan and Hynynen, 1996) and Wan et al. (1999). With proper optimization, the treatment time can be decreased and heating can be better localized in both healthy and cancerous tissue.

In ultrasound surgery, the optimization is usually made for the thermal dose rather than the temperature. By controlling the thermal dose directly, the peak temperature in tissue can be decreased which results in decreased applied power and treatment time (Daum and Hynynen, 1998). The proposed thermal dose optimization methods include power adjusted focus scans Wan et al. (1996), direct search algorithms for thermal dose weighting (Hutchinson, Dahleh and Hynynen, 1996) and temporal switching between multiple focus patterns (Daum and Hynynen, 1998) and (Fjield and Hynynen, 1997). In above studies, optimization routines were rather simple and optimization was accomplished by choosing between a few preselected strategies. The more sophisticated routine for thermal dose optimization was proposed in Wan et al. (1999). That method uses the Gaussian approximation for the thermal dose distribution with a two step optimization routine. The main limitation of the method is that optimization was accomplished between the pre determined foci in 1D. Finally, the model predictive control (MPC) method was derived in (Arora, Skliar and Roemer, 2002). In MPC approach, thermal dose is linearized and quadratic cost criteria is used to weight the thermal dose. In that approach, the modeling errors can be decreased using the temperature feedback during the treatment. In addition, inequality constraints can be used for limiting the temperature during the sonication. The main draw backs of the MPC approach are that it is based on the predetermined focus points and scanning path, and it is computationally expensive, especially in 2D and 3D.

In this paper, an alternative method for thermal dose optimization is presented. Method can be divided to two parts. In the first part, the model based optimization is used to determine phases and amplitudes of the ultrasound transducers to optimize the temperature or thermal dose in tissue. The method is based on the optimal control theory, and it uses

quadratic cost criteria for the desired thermal dose and inequality constraints for the maximum applied amplitude. This approach results in large dimension nonlinear control problem. The proposed method is not based on the predetermined focus points or scanning path, i.e. phase and amplitude are changed as a function of time to produce the desired thermal dose. With proposed method, the thermal dose can be optimized in both healthy and cancerous tissue. The details of the proposed method can be found from (Malinen, Huttunen and Kaipio, 2003a) for temperature optimization and from (Malinen, Huttunen and Kaipio, 2003b) and Malinen et al. (2004) for thermal dose optimization. In the second part of the overall method, LQG feedback controller and Kalman filter are derived by linearizing the original nonlinear control problem with respect to the optimized trajectories for temperature and phase and amplitude. This feedback controller can be applied during the actual sonication when temperature is measured with MRI. The purpose of the feedback controller is to decrease the effect of the modeling errors which may appear in model based optimization. The details of the feedback controller can be found from Malinen et al. (2005). The potential of the proposed methods is shown with numerical simulations in 2D.

2. Physical models and computational approximations

2.1 Helmholtz equation

The time harmonic ultrasound field is the solution of the Helmholtz equation in an inhomogeneous medium

$$\nabla \cdot \left(\frac{1}{\rho}\nabla p\right) + \frac{\kappa^2}{\rho} p = 0, \tag{1}$$

where ρ is density, c is the speed of sound and κ is the wave number. In dissipative media the wave number is defined as $\kappa = 2\pi f/c + i\alpha$ where f is the frequency of the wave field and α is the absorption coefficient (Bhatia, 1967).

Since standard finite element and finite difference methods for the Helmholtz problem (1) need extremely dense meshes at ultrasound frequencies, alternative approaches have been proposed. In such approaches, a priori information is included to the approximation subspace. These methods include partition of unity method (PUM) (Babuška, and Melenk, 1997), least squares method (Monk and Wang, 1999) and ultra weak variational formulation (UWVF) (Cessenat and Després, 1998) and (Cessenat and Després, 2003). In this paper, the Helmholtz equation is solved with the UWVF. In following, the UWVF approximation of the Helmholtz equation is outlined.

We partition the domain of interest Ω with disjoint finite elements Ω_j and let ν_j be the outward unit normal for j'th element. In addition, let the boundary between elements Ω_j and Ω_ℓ be $\Sigma_{j\ell}$. If the element Ω_j is on the boundary of the domain Ω, the coinciding boundary is denoted by $\partial\Omega_j \cap \partial\Omega = \Gamma_j$.

If the material parameters ρ and c are approximated with piecewise constant functions we can decompose the Helmholtz problem for all $1 \leq j \leq K$ as

$$\Delta p_j + \kappa_j^2 p_j = 0 \quad \text{in } \Omega_j \tag{2}$$

$$\frac{1}{\rho_j}\frac{\partial p_j}{\partial \nu_j} - i\sigma p_j = -\frac{1}{\rho_\ell}\frac{\partial p_\ell}{\partial \nu_\ell} - i\sigma p_\ell \quad \text{on } \Sigma_{j\ell} \tag{3}$$

$$\frac{1}{\rho_j}\frac{\partial p_j}{\partial \nu_j} - i\sigma p_j = \tau\left(-\frac{1}{\rho_j}\frac{\partial p_j}{\partial \nu_j} - i\sigma p_j\right) + g \quad \text{on } \Gamma_j \tag{4}$$

where $p_j = p|_{\Omega_j}$ $\tau \in \mathbb{C}$, $|\tau| \leq 1$, and the coupling parameter $\sigma > 0$, $\sigma \in \mathbb{R}$. The source term is denoted by g. By adjusting parameters τ and σ a wide range of boundary conditions can be obtained on Γ_j.

Next step is to define the function f, $f|_{\partial\Omega_j} = f_j$ on the element boundaries as follows

$$f_j = \left(\left(-\frac{1}{\rho_j}\frac{\partial}{\partial \nu_j} - i\sigma\right)p_j\right)\Bigg|_{\partial\Omega_j}, \quad 1 \leq j \leq K. \tag{5}$$

It is shown in (Cessenat and Després, 1998) and (Huttunen, Monk and Kaipio, 2002) that f_j satisfies the ultra weak variational formulation, which is

$$\begin{aligned}\sum_{j=1}^{K}\int_{\partial\Omega_j}\frac{1}{\sigma}f_j\overline{\left(-\frac{1}{\rho_j}\frac{\partial}{\partial \nu_j} - i\sigma\right)q_j} - \sum_{j=1}^{K}\sum_{\ell=1}^{K}\int_{\Sigma_{j\ell}}\frac{1}{\sigma}f_\ell\overline{\left(\frac{1}{\rho_j}\frac{\partial}{\partial \nu_j} - i\sigma\right)q_j} - \sum_{j=1}^{K}\int_{\Gamma_j}\frac{\tau}{\sigma}f_j\overline{\left(\frac{1}{\rho_j}\frac{\partial}{\partial \nu_j} - i\sigma\right)q_j} \\ = \sum_{j=1}^{K}\int_{\Gamma_j}\frac{1}{\sigma}g\overline{\left(\frac{1}{\rho_j}\frac{\partial}{\partial \nu_j} - i\sigma\right)q_j},\end{aligned} \tag{6}$$

for all test functions q_j which are the solutions of the adjoint Helmholtz equation $\Delta\overline{q}_j + \kappa_j^2\overline{q}_j = 0$ in Ω_j, where the overbar denotes complex conjugation.

Expressing the solutions in each element as a linear combination of appropriate plane wave basis functions (N_k basis functions in element Ω_k) and using these basis functions also as test functions (Galerkin approach), the problem can be written in the form of the matrix equation

$$(I - D^{-1}C)X = D^{-1}b, \tag{7}$$

where the unknowns $X = (f_{11}, \ldots, f_{KN_K})^T$ are to be determined. The matrices D and C are sparse and exhibit block structure. To avoid conditioning problems, we allow the number of bases N_j to vary between the elements (Huttunen, Monk and Kaipio, 2002).

2.2 Bioheat equation

The temperature evolution in tissues can be characterized with Pennes bioheat equation (Pennes, 1948)

$$\rho C_{\mathrm{T}} \frac{\partial T}{\partial t} = \nabla \cdot k \nabla T - w_{\mathrm{B}} C_{\mathrm{B}} (T - T_{\mathrm{A}}) + Q\,, \tag{8}$$

where T is the temperature, C_{T} is the heat capacity of tissue, k is the diffusion coefficient, w_{B} is the arterial perfusion, C_{B} is the heat capacity of blood, T_{A} is the arterial blood temperature and Q is the heat source term. The heat source term for the time-harmonic acoustic pressure is (Pierce, 1994)

$$Q = \frac{\alpha |p|^2}{\rho c}. \tag{9}$$

In this paper, the bioheat equation is solved with Galerkin type FEM. The FEM formulation of the bioheat equation and the rearranging of the heat source term is discussed in detail in (Malinen, Huttunen and Kaipio, 2003a) and (Malinen, Huttunen and Kaipio, 2003b). In this paper, the time integration of the bioheat equation is computed with implicit Euler integration. The implicit Euler FEM form of the Eq. (8) is

$$T_{t+1} = A_t T + P + M_{\mathrm{D}} (B u_t)^2, \tag{10}$$

where matrix $A \in \mathbb{R}^{N \times N}$ comes from the standard theory of FEM, vector $P \in R^N$ comes from the perfusion term and $M_D \in \mathbb{R}^{N \times 2N}$ is the modified mass matrix. The matrix $B \in \mathbb{R}^{2N \times 2m}$ is constructed from m separated ultrasound fields so that the imaginary and the real parts of each field are separated. The optimization input vector $u_t \in \mathbb{R}^{2m}$ is constructed from time varying coefficients for each real and imaginary part. In the FEM solution, the temperature in the boundary of the computation domain is set to 37° with the Dirichlet condition.

2.3 Thermal dose

The effect of the temperature and the treatment time can be characterized with the thermal dose D. For biological tissues thermal dose is defined as (Sapareto and Dewey, 1984)

$$D = \int_0^{t_f} R^{\left(43 - T(t)\right)}\, dt\,, \quad \text{where } R = \begin{cases} 0.25 & \text{for } T(t) < 43^{\circ}\mathrm{C} \\ 0.50 & \text{for } T(t) \geq 43^{\circ}\mathrm{C} \end{cases}, \tag{11}$$

where t_f is the final time where thermal dose is integrated. The unit of the thermal dose is equivalent minutes at 43°C. In most of the soft tissues the thermal dose that causes necrosis is reported to be between 50 and 240 equivalent minutes at 43°C (Damianou and Hynynen, 1994) and (Damianou, Hynynen and Fan, 1995).

3. Optimization and control algorithms

3.1 Model based thermal dose optimization method

The cost function for thermal dose optimization can be defined as

$$J(T, \dot{u}) = \frac{1}{2}(D(T) - D_d)^T W (D(T) - D_d) + \frac{1}{2} \int_0^{t_f} \dot{u}_t^T S \dot{u}_t \, \mathrm{d}t, \tag{12}$$

where the difference between the desired thermal dose D_d and the current thermal dose D is weighted with a positive definite matrix W and the time derivative of the control input $\dot{u}_t$ is weighted with a positive definite matrix S.

The maximum input amplitude of the ultrasound transducers is limited. This limitation can be handled with inequality constraint approximation, which i^{th} component can be written as

$$c_i(u_t) = \tag{13}$$
$$\begin{cases} K\left((u_{i,t}^2 + u_{m+i,t}^2)^{1/2} - u_{\max,\mathrm{k}}\right)^2, & \text{if} \quad \left(u_{i,t}^2 + u_{m+i,t}^2\right)^{1/2} \geq u_{\max,\mathrm{k}} \\ 0, & \text{if} \quad \left(u_{i,t}^2 + u_{m+i,t}^2\right)^{1/2} < u_{\max,\mathrm{k}} \end{cases}$$

where K is the weighting scalar and $u_{\max,\mathrm{k}}$ is the maximum amplitude during k^{th} interval of the treatment.

Next step is to define the Hamiltonian for the problem (Stengel, 1994). Combining the state equation (10), cost function (12) and inequality constraint approximation (13) gives the Hamiltonian

$$\begin{aligned} H(T,u,\dot{u}) &= \frac{1}{2}(D(T)-D_d)^T W(D(T)-D_d)+\frac{1}{2}\dot{u}_t^T S\dot{u}_t \\ &\quad +\lambda_t^T\left(AT_t-P-M\big(Bu_t\big)^2\right)+\mu_t^T c\big(u_t\big)\,, \end{aligned} \tag{14}$$

where λ_t is the Lagrange multiplier for the state equation and μ_t is the Lagrange multiplier for the input amplitude inequality constraint approximation.

The solution to the optimization problem is computed with the gradient search algorithm from which the details can be found from (Malinen, Huttunen and Kaipio, 2003b) and Malinen et al. (2004). The algorithm consists of the following steps: 1) Compute the state equation (10). 2) Compute the Lagrange multiplier for the state equation as $\lambda_t = \partial H/\partial T_t$ in Eq. (14). 3) Compute the Lagrange multiplier for the input inequality constraint from Equations (13) and (14) as $\mu_t = (\partial c/\partial u_t)^{-1}(\partial H/\partial u_t)$. 4) Compute the stationary condition (i.e. $\partial H/\partial u_t$). 5) Compute the update for the input at iteration round ℓ as $u^{\ell+1} = u^\ell + \epsilon(\partial H/\partial u_t)^\ell$, where ϵ is the step length. 6) If the change in the cost function (12) is small enough, stop iteration, else return to the step 1).

3.2 Feedback controller for temperature

The modeling errors in model based optimization affects the obtained temperature and thermal dose distribution. The modeling errors are mainly in the acoustic parameters of the Helmholtz equation and in the thermal parameters of the bioheat equation. To compensate these errors during the treatment, the MRI based temperature feedback can be used on line during the treatment. In this study, the LQG feedback controller and Kalman filter are used for feedback control and state estimation.

The feedback controller can be derived by linearizing the nonlinear state equation (10) with respect to the optimized temperature and input trajectories. At this stage, the time discretization is also changed, since model based optimization is computed with the time discretization of the order of a second, while MRI imaging sequences are few seconds during the ultrasound surgery.

Let the length of the time discretization in model based optimization be h. In feedback control d steps of model based optimization control are taken at once, giving new step length dh. With these changes, the linearized multi-step state equation can be written as

$$\Delta T_{k+1} = \widetilde{F}\Delta T_k + \widetilde{B}_k\Delta u_k\,, \quad \text{where } \widetilde{F} = A^d, \quad \widetilde{B}_k = h\sum_{t=kd+1}^{kd+d} A^{t-kd-1}G(u_{0,t}) \tag{15}$$

and where $G(u_{0,t})$ is the Jacobian matrix of the state equation with respect to the model based optimization input trajectory $(u_{0,t})$, ΔT_{k+1} is the linearized temperature and Δu_k is the feedback correction to the input. The cost function for the LQG control can be set as

$$\Delta J = \sum_{k=1}^{N_k}\left((\Delta T_k)^T\,Q\,(\Delta T_k)+\Delta u_k^T\,R\,\Delta u_k\right)\,. \tag{16}$$

where positive definite matrix Q weights the linearized temperature (i.e. difference between actual temperature and optimized temperature) and positive definite matrix R weights the LQG input correction.

The LQG feedback controller and the Kalman filter gains are computed from the standard optimal control theory (Stengel, 1994) by solving the associated Riccati matrices (for details, see Malinen et al. (2005)).

In this study, the LQG feedback control and Kalman filter are tested using simulated data. In model based optimization, the acoustic and thermal parameters are adopted from the literature and they are known only approximately. In simulations, different thermal parameters are used when real system is simulated. In this case the bioheat equation can be written as

$$T_{t+1} = A_rT_t + P_r + M_{D,r}(B_r(u_{0,t}+\Delta u_k))^2, \tag{17}$$

where the feedback correction Δu_k is held constant over the time interval $t \in [k, k+1]$ and subscript r denotes associated FE matrices which are constructed using the real parameters. In addition, the state estimate is computed with the same discretization (with step length h) as the state equation with original optimization control matrices, since errors are considered as unknown disturbances to the system. During the time interval $t \in [k, k+1]$, the state estimate is

$$\widehat{T}_{t+1} = A\widehat{T}_t + P + M_D(B(u_{0,t}+\Delta u_k))^2. \tag{18}$$

The corrections for the state estimate and the input are updated after every step k from the measurements and the state estimated feedback using

$$y_k = CT_k + v_k \tag{19}$$

$$\widehat{T}_{k+1} = A\widehat{T}_k + P + M_D\big(B(u_{0,k} + \Delta u_k)\big)^2 + L(y_k - C\widehat{T}_k) \tag{20}$$

$$\Delta u_{k+1} = -K_{k+1}(\widehat{T}_{k+1} - T_{0,k+1})\,, \tag{21}$$

where y_k is the measurement, v_k is the measurement noise, L is the steady state Kalman gain and K_{k+1} is the time-varying LQG feedback gain. The feedback correction is constant during time interval $t \in [k, k+1]$ and piece wise constant during the whole treatment.

4. Numerical studies

The model problem concerns ultrasound surgery of the breast cancer. The computational domain is shown in Fig. 1. The domain is divided into four subdomains which are water (Ω_1), skin (Ω_2), healthy breast (Ω_3) and cancer (Ω_3). The transducer system which was used in simulations was a 20-element phased array on the left side of the domain. The acoustic and thermal parameters for subdomains are given in Table 1. The heat capacity of blood was set to 3770 J/kgK in all simulations. The computational domain was divided into mesh with 2108 nodes and 4067 elements.

Table 1. The acoustic and thermal parameters for the model based optimization.

Domain	α (Nep/m)	c (m/s)	ρ (kg/m^{3}s)	k (W/mK)	C_{T} (J/kgK)	w_{B} (kg/m^{3}s)
Ω_1	0	1500	1000	0.60	4190	0
Ω_2	12	1610	1200	0.50	3770	1
Ω_3	5	1485	1020	0.50	3550	0.7
Ω_4	5	1547	1050	0.65	3770	2.3

The frequency of the wave fields was set to 500 kHz. The ultrasound fields were computed with the UWVF for each transducer element. The solutions were normed so that the maximum amplitude was 1 MPa for all ultrasound fields.

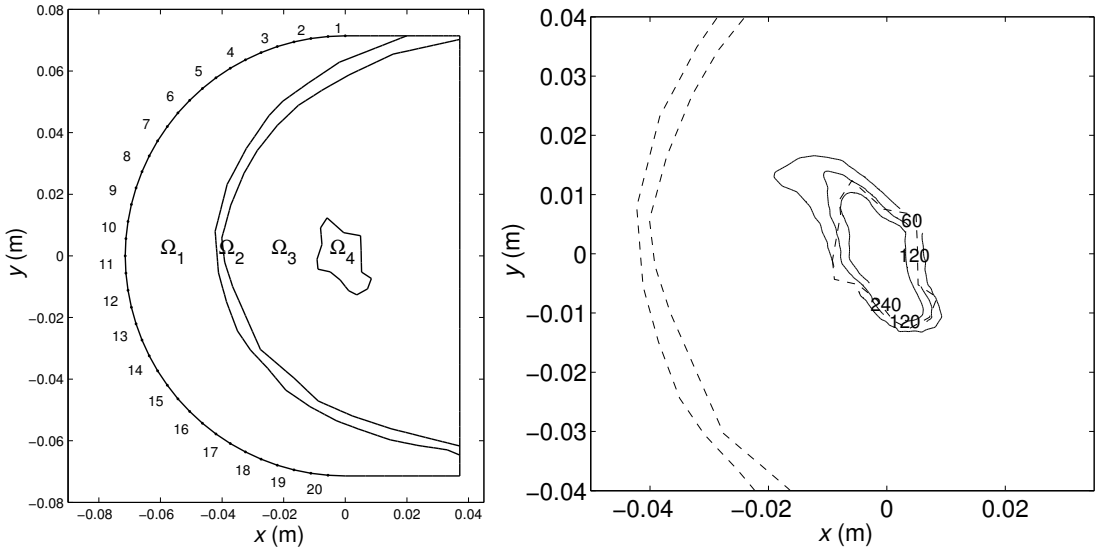

Figure 1. Left: The computing domain with 20 ultrasound transducers located in the left (numbered $1, \ldots, 20$). Right: thermal dose contours from the model based optimization in the region of interest.

The optimization problem was to achieve the thermal dose of 240 equivalent minutes at 43°C in cancer area while keep the thermal dose in healthy tissue below 120 equivalent minutes. Treatment time was set to 180 s and time step h was 0.5 s in temporal discretization. The weighting matrix W for the thermal dose was set to a diagonal matrix. The weights were set to 500 for the nodes in the skin (Ω_2), 2500 for the nodes in the breast (Ω_3) and 2000 for the nodes in the cancer region (Ω_4). The nodes in the water (Ω_1) were weighted with zero.

The input inequality constraint approximation was set for the maximum amplitude $u_{\max,1}$=0.8 MPa for $t = [0, \ldots, 50]$ s and $u_{\max,2}$=0.02 MPa for $t = [50, \ldots, 180]$ s. These criteria mean that when the transducers are on, the amplitude is

limited by $u_{\max,1}$, and when the transducers are effectively turned off, the amplitude is limited by $u_{\max,2}$. The inequality constraint weighting was set as $K = 60000$. Another design criteria for input was that these trajectories was desired to be non-oscillating functions of time. This criterion was satisfied by setting weighting matrix S$= \mathrm{diag}(10000)$ for time derivative of the input. The iteration step parameter ϵ was chosen so that the point wise correction to the input was less than 0.01 MPa. The thermal dose was optimized with algorithm described in subsection 3.1. The stopping criterion in this case was that the relative change in cost function was less than 10^{-5}. With these parameters, it took 1200 rounds to satisfy the stopping criterion.

The resulting thermal dose contours for the region of the interest is shown in Fig. 1. This figure indicates that the major part of the dose is in the cancerous area, while healthy regions does not suffer from significant thermal damage. The thermal dose of 240 equivalent minutes is achieved in 74.5% of the cancer area, while thermal dose in other regions is reasonable low. The thermal dose of 120 equivalent minutes can be found only from 2.4% of the healthy breast while dose in skin is much lower than 120 equivalent minutes. These results indicate that the design criteria is approximately valid in all subdomains.

Examples of the phase and amplitude trajectories are shown in Fig 2. The amplitude was limited effectively to 0.8 MPa with inequality constraint approximation during the first part of the treatment and to 0.02 MPa during the second part, i.e. when tissue cools. The cooling time is crucial in this problem, since 75% of the thermal dose was accumulated during the cooling period. Finally, there is no oscillation in phase and amplitude trajectories so the non-oscillatory penalty is also satisfied.

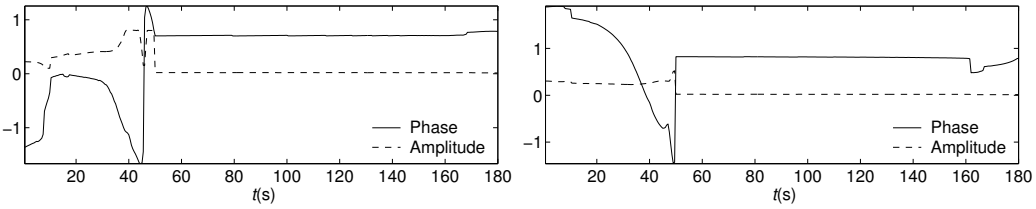

Figure 2. The phases and the amplitudes of the transducer signals from the optimization control simulation. The figures are for the transducer 3 (left) and 15 (right).

4.1 Feedback control simulations

The LQG feedback controller and Kalman filter were also numerically tested. The time lag between the temperature measurements was chosen to be 4 s to simulate the MRI imaging sequences. The temperature measurement at each vertex in the mesh was taken as the mean value of the computed temperature over each 4 s interval. The multi-step implicit Euler was adopted by setting d=8 corresponding to a lag of dh=4 s. The LQG feedback controller was derived by choosing the temperature trajectory weighting matrix to $Q = W/1000$ and the weighting for the input correction Δu_k was set $R =$diag(1000). In simulations, Gaussian noise with standard deviation of $\pm 1^{\circ}$C was added to the temperature measurements.

In following, results from the worst case simulation are presented. This example was chosen to simulate the real system whose acoustic and thermal parameters are not known exactly. In feedback simulation, the absorption in tissues is dramatically higher than in model based optimization. In addition, other acoustic and thermal parameters are also changed.

The acoustic and thermal parameters for feedback simulation are given in Table 2. The wave fields were solved with UWVF using given parameters. The thermal dose contours with and without feedback are shown in Fig. 3. The higher

Table 2. The acoustic and thermal parameters for the feedback control simulation.

Domain	α (Nep/m)	c (m/s)	ρ (kg/m^{3}s)	k (W/mK)	C_{T} (J/kgK)	w_{B} (kg/m^{3}s)
Ω_{II}	14	1700	1100	0.60	3650	0.8
Ω_{III}	7	1500	980	0.70	3600	0.6
Ω_{IV}	8	1400	1000	0.70	3700	2.0

thermal dose contours without feedback covers large area of the healthy breast, while LQG feedback decreases undesired thermal dose effectively.

The temperature trajectories from feedback simulation are shown in Fig. 4. This figure indicates that feedback controller effectively decreases the maximum temperature in both healthy and cancerous tissue, i.e. feedback controlled temperature trajectories follows optimized trajectories with tolerable accuracy.

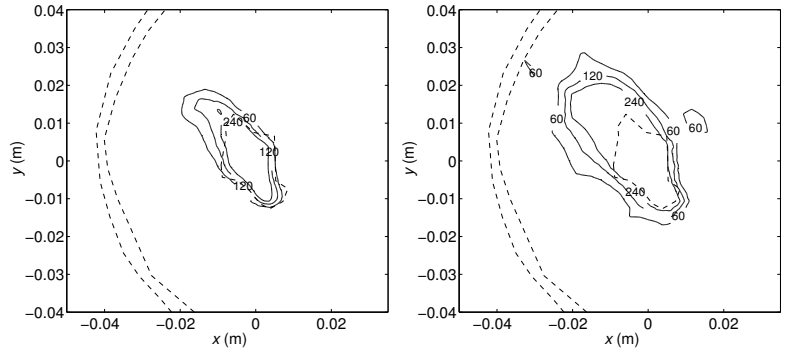

Figure 3. Thermal dose contours from the feedback simulation. Left: Thermal dose contours with feedback. Right: Thermal dose contours without feedback.

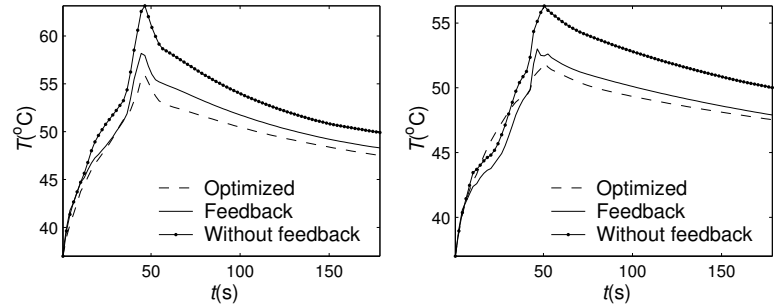

Figure 4. Results from the feedback simulation. Left: The maximum temperature in the cancer (Ω_4). Right: The maximum temperature in the healthy breast (Ω_3).

5. Conclusions

In this paper, the two-stage optimization method for ultrasound surgery was proposed. The proposed method was tested with numerical simulations in 2D for model based optimization and feedback cases.

The main advantages of the proposed model based optimization method is that it changes the phase and amplitude of the ultrasound transducers as a function of time to obtain the desired thermal dose. This is an advantage as compared to methods which uses predetermined focus points and scanning path. In proposed method, the thermal dose can be optimized in both healthy and cancerous tissue and method takes into account diffusion and perfusion during the treatment. Furthermore, thermal dose accumulation during the cooling is also taken into account.

The proposed feedback controller can change not only amplitude but also the phase of the ultrasound transducers. This is a clear advantage when inhomogeneous modeling errors are present. The phase correction is necessity to compensate this kind of errors.

The numerical simulations of the proposed methods show that the thermal dose can be accurately localized to target region. In addition, the feedback controller can compensate large modeling errors, which increases the clinical potential of the overall method.

Finally, the proposed model based optimization scheme is also extended to 3D in Malinen et al. (2004). In that study the inequality constraints for the temperature in both healthy and cancerous tissue are also introduced.

6. References

Arora, D., Skliar, M. and Roemer, R.B., 2002, "Model-predictive control of hyperthermia treatments" IEEE Transactions on Biomedical Engineering, Vol 49, pp. 629–639.

Babuška, I., and Melenk, J.M., 1997, "The partition of unity method" International Journal for Numerical Methods in Engineering, Vol.40, pp. 727–758.

Bhatia, A.B., 1967, "Ultrasonic Absorption: An Introduction to the Theory of Sound Absorption and Dispersion in Gases, Liquids and Solids" Dover.

Cessenat, O. and Després, B., 1998, "Application of an ultra weak variational formulation of elliptic PDEs to the two-dimensional Helmholtz problem", SIAM Journal of Numerical Analysis, Vol.35,No. 1, pp. 255–299.

Cessenat, O. and Després, B., 2003, "Using plane waves as base functions for solving time harmonic equations with the

ultra weak variational formulation", Journal of Computational Acoustics, Vol. 11, No. 2, pp. 227–238.

Cline, H.E., Schenk, J.F., Watkins, R.D., Hynynen, K. and Jolesz, F.A., 1993, "Magnetic resonance-guided thermal surgery", Magnetic Resonance in Medicine, Vol. 30, pp. 98–106.

Damianou C. and Hynynen, K., 1994, "The effect of various physical parameters on the size and shape of necrosed tissue volume during ultrasound surgery", The Journal of the Acoustical Society of America, Vol. 95, No. 3, pp. 1641–1649.

Damianou, C.A. Hynynen, K. and Fan, X., 1995, "Evaluation of accuracy of a theoretical model for predicting the necrosed tissue volume during focused ultrasound surgery." IEEE Transactions on Ultrasonics, Ferroelectrics and Frequency Control, Vol. 42, No. 2, pp. 182–187.

Daum, D.R. and Hynynen, K., 1998, "Thermal dose optimization via temporal switching in ultrasound surgery", IEEE Transactions on Ultrasonics, Ferroelectrics, and Frequency Control, Vol. 45, No. 1, pp. 208–215.

Fan, X. and Hynynen, K., 1996, "Ultrasound surgery using multiple sonications – treatment time considerations", Ultrasound in Medicine and Biology, Vol. 22, pp. 471–482.

Fjield, T. and Hynynen, K., 1997, "The combined concentric-ring and sector-vortex phased array for MRI guided ultrasound surgery", IEEE Transactions on Ultrasonics, Ferroelectrics and Frequency Control, Vol. 44, pp. 1157–1167.

Hutchinson, E.B., Dahleh, M. and Hynynen, K., 1996, "MRI feedback control for phased array prostate hyperthermia", In Proceedings of the IEEE Ultrasonics Symposium, pp. 1285–1288.

Huttunen, T., Monk, P. and Kaipio, J.P., 2002, "Computational aspects of the ultraweak variational formulation", Journal of Computational Physics, Vol. 182, pp. 27–46.

Hynynen, K., 1996, "Focused ultrasound surgery guided by MRI", Science & Medicine, September/October, pp. 62–71..

Malinen, M., Duncan, S.R., Huttunen, T. and and Kaipio, J.P., 2005, "Feedforward and feedback control of the thermal dose in ultrasound surgery", Applied Numerical Mathematics, In press.

Malinen, M. Huttunen, T., Hynynen, K., and Kaipio, J.P., 2004, "Simulation study for thermal dose optimization in ultrasound surgery of the breast", Medical Physics, Vol. 31, pp. 1296–1307.

Malinen, M., Huttunen, T. and Kaipio, J.P., 2003a, "An optimal control approach for ultrasound induced heating", International Journal of Control, Vol. 76, pp. 1323–1336.

Malinen, M., Huttunen, T. and Kaipio, J.P., 2003b, "Thermal dose optimization method for ultrasound surgery", Physics in Medicine and Biology, Vol. 48, pp. 745–762.

Monk, P. and Wang, D., 1999, "A least squares method for the Helmholtz equation", Computer Methods in Applied Mechanics and Engineering, Vol. 175, pp. 121–136.

Pennes, H.H., 1948, "Analysis of tissue and arterial blood temperatures in the resting human forearm", Journal of Applied Physiology, Vol. 1, pp. 93–122.

Pierce, A.D., 1994, "Acoustics: An Introduction to its Physical Principles and Applications", Acoustical Society of America.

Sapareto, S.A. and Dewey, W.C., 1984, "Thermal dose determination in cancer therapy", International Journal of Radiation Oncology, Biology, Physics, Vol 10, No. 6, pp. 787–800.

Stengel, R.F., 1994, "Optimal Control and Estimation", Dover.

ter Haar, G., 1995, "Ultrasound focal beam surgery", Ultrasound in Medicine and Biology, Vol. 21, No. 9, pp. 1089–1100.

ter Haar, G., 2001, "Acoustic surgery", Physics Today, December, pp. 29–34.

Wan, H., Aarsvold, J., O'Donnel, M., and Cain, C., 1999, "Thermal dose optimization for ultrasound tissue ablation", IEEE Transactions on Ultrasonics, Ferroelectrics and Frequency Control, Vol. 46, No. 6, pp. 913–928.

Wan, H., VanBaren, P., Ebbini, E.S. and Cain, C.A., 1996, "Ultrasound surgery: Comparison of strategies using phased array systems", IEEE Transactions on Ultrasonics Ferroelectrics, and Frequency Control, Vol. 43, No. 6, pp. 1085–1098.